



Diffusion-Weighted Imaging and Proton Magnetic Resonance Spectroscopy Findings in Osteosarcoma Versus Normal Muscle

Mahrooz Malek,¹ Mohamad Ali Kazemi,^{1*} Sadegh Saberi,² Hassan Hashemi,¹ and Behnaz Moradi¹

¹Advanced Diagnostic and Interventional Radiology Research Center (ADIR), Medical Imaging Center, Imam Khomeini Hospital Complex, Tehran University of Medical Sciences, Tehran, Iran

²Department of Orthopedic Surgery, Imam Khomeini Hospital Complex, Tehran University of Medical Sciences, Tehran, Iran

*Corresponding author: Mohamad Ali Kazemi, Advanced Diagnostic and Interventional Radiology Research Center (ADIR), Medical Imaging Center, Imam Khomeini Hospital Complex, Tehran University of Medical Sciences, Tehran, Iran. Tel: +98-9131044663, E-mail: ma-kazemi@sina.tums.ac.ir

Received 2016 April 19; Revised 2017 February 10; Accepted 2017 March 11.

Abstract

Objectives: The goal of our study was to assess diffusion-weighted (DW) imaging and proton magnetic resonance (MR) spectroscopy findings in osteosarcoma versus normal muscle at 3 Tesla (3 T) MR system.

Patients and Methods: Nineteen patients highly suspicious for osteosarcoma and 12 normal young healthy adults were enrolled in this study. Two patients were excluded from the study due to incompatible histopathologic results. DW imaging and multivoxel proton MR spectroscopy at 3 T were performed for all participants. Surgical biopsy and histopathological examination were done for every patient after imaging. SPSS 20 was used for statistical analysis.

Results: The minimum apparent diffusion coefficient (ADC) value of osteosarcoma (0.88 ± 0.28) in this study confirms the significant restriction of this tumor against the dark background of normal muscle in high b-value images. Fourteen (82%) of the available 17 patients had ADC values $\leq 1 \times 10^{-3} \text{ mm}^2/\text{s}$. The maximum choline/creatine (Cho/Cr) ratio of osteosarcoma (1.94 ± 1.12) was statistically higher than the normal muscle (1.34 ± 0.11). Receiver operating curve (ROC) analysis (the area under the curve = 0.7) indicated a maximum Cho/Cr ratio of 1.37 as the cut point between the normal muscle and osteosarcoma, with a sensitivity, specificity and accuracy of 58.8%, 83.3%, and 69%, respectively. All patients with Cho/Cr ratios more than the cut point had ADC values $\leq 1 \times 10^{-3} \text{ mm}^2/\text{s}$ and all patients with ADC values higher than $1 \times 10^{-3} \text{ mm}^2/\text{s}$ had Cho/Cr ratios ≤ 1.37 .

Conclusion: It was concluded that DW imaging and proton MR spectroscopy are two effective noninvasive techniques in the evaluation of osteosarcoma.

Keywords: Diffusion-Weighted Imaging, Proton MR Spectroscopy, Osteosarcoma, Normal Muscle

1. Background

Osteosarcoma is among the most common primary bone tumors that occur predominantly in children and young adults (1). The tumor is classified into a variety of histological subtypes and mostly involves metaphyseal regions of the distal femur, proximal tibia and proximal humerus (2).

A variety of imaging techniques have been recommended for evaluation of osteosarcoma including computed tomography, radionuclide bone scanning, plain-film radiography, and magnetic resonance imaging (MRI) (3). MRI is widely used in the assessment of musculoskeletal lesions, though it has limitations in distinguishing involved from non-involved areas (4, 5).

Novel and advanced imaging modalities such as proton magnetic resonance (MR) spectroscopy and diffusion-weighted imaging (DWI) have emerged as important tools for improving diagnostic accuracy and specificity (6).

Proton MR spectroscopy is a novel diagnostic approach that can characterize the tissue metabolites and malignant activity in a noninvasive manner (7, 8). Proton MR spectroscopy has been used in a wide variety of cancer types, including bone and soft tissue tumors, breast and prostate cancers (9). Its effectiveness to distinguish musculoskeletal malignant and benign lesions by measuring choline-containing compounds has been the focus of the recent investigations (5, 7). Indeed, in a variety of malignant tumors, elevated levels of choline/creatine (Cho/Cr) ratios have been identified as indicators of accelerated cell-membrane turnover (10). So that abundant levels of choline metabolites as an indirect marker of malignancy are present in malignant musculoskeletal lesions (11). Recent studies have demonstrated that MR spectroscopy with metabolite quantification is helpful for characterizing musculoskeletal lesions (5, 12).

An appealing alternative MRI technique and recent ad-

dition to the musculoskeletal MR sequences is DWI. DWI is a functional imaging method that measures the brownian motion of water molecules within a voxel of tissue (13, 14). Extracellular water molecules have relatively unimpeded motion compared to intracellular water molecules (15). Restriction of water molecules mobility is greater in highly cellular tissues (tumors). Therefore, DWI can aid in differentiating normal from pathological situations (13). Current literature has suggested that DW imaging can provide valuable information to assess osteosarcoma (16). DWI provides a quantitative analysis via the apparent diffusion coefficient (ADC): low ADC value in highly cellular sites and high ADC value in low cell density sites.

Indeed, there is little information on the role of DW imaging in characterizing primary bone tumors. In light of this consideration, more studies are required to clarify the potential utility, accuracy and role of DWI and proton MR spectroscopy over conventional sequences in characterizing musculoskeletal tumors.

2. Objectives

The purpose of this study was to measure and compare Cho/Cr ratios and ADC values in osteosarcoma versus normal group in order to be used in osteosarcoma evaluation and as a preliminary report to reach the final goal of demarcating normal from tumoral tissues in patients with osteosarcoma.

3. Patients and Methods

3.1. Ethics Statement

The study protocol was approved by the ethics committee of Tehran University of Medical Sciences and institutional review board of the Imam Khomeini university hospital. Written informed consent was obtained from all participants prior to examination.

3.2. Participants

Between August 2013 and November 2014, 19 patients highly suspicious of osteosarcoma, according to their plain films, and 12 normal young healthy adults were enrolled in this study. Before imaging, none of the patients received treatment and no interventional procedures such as aspiration or biopsy were performed on the tumors. Surgical biopsy and histopathological examination were done for every patient after imaging. Two patients with histopathologic diagnosis other than osteosarcoma were excluded from the study. The mean age of the remaining 17 patients (10 males, 7 females) was 25.3 years with age ranges

of 15 to 30 with the exception of a 59-year-old woman. Normal healthy adults (six males, six females) were in the age range of 22 to 29 years (mean age, 25.9 years).

3.3. Radiological Assessment

3.3.1. Proton Magnetic Resonance (MR) Spectroscopy

Patients and normal groups were examined with the similar protocol and same 3-T MR system. Since thigh and arm are common sites of osteosarcoma, these sites of the normal group were examined as well. No abnormal signal was observed in conventional images of this group.

All examinations were performed at a 3 T superconducting MR imaging unit (Magnetom Tim Trio; Siemens, Erlangen, Germany) using high performance gradients and phased-array surface coils. The conventional MR imaging, as anatomical imaging, was consisted of axial, coronal, and sagittal proton density (PD)-weighted spin-echo sequence (repetition time (TR) ms/echo time (TE) ms, 3100/32; slice thickness, 6mm; flip angle, 90°; number of excitation, 1; scan time, 200s). Spectra of two-dimensional (2D) multivoxel proton MR spectroscopy were obtained by employing the point-resolved spectroscopic sequence (PRESS) (TR/TE, 2500 ms/135 ms; band width, 1200; average, 16; number of data points, 1024). We used phased-array surface coils to reach higher signal to noise ratios.

In patients, the volume of interest (VOI) was placed within the tumoral tissue, and detected on PD images. Based on acquiring an appropriate coverage of the mass and each voxel size reaching $15 \times 15 \times 15 \text{ mm}^3$, the field of view (FOV) and number of voxels in each direction were selected. In the normal group, the VOI was inserted in the normal muscle anatomy in the thigh or arm, and each voxel size was the same as the patients group. We did not need to suppress lipid because of enough suppression in TE of 135, but water suppression was applied (8). Choline, creatine, water, lipid and N acetyl aspartate (NAA) peaks were defined. Automatic and manual shimming was carried out to optimize the field homogeneity. Frequency, transmitter, shim and water suppression adjustment were performed before data collection. The voxel with maximum Cho/Cr ratio was selected. In patients, this voxel had to be entirely within obvious tumoral tissue and in the normal group, it had to be completely within the normal muscle. Any contamination with adjacent tissue, artifact and significant noisy spectra were not accepted. Discrete choline and creatine peaks had to be present. The Cho/Cr ratio of this voxel was registered for each subject.

3.3.2. Diffusion-Weighted Imaging

DW imaging was performed in coronal or axial orientation by employing a spin echo echoplanar imaging

sequence (TR/TE, 900 ms/80 ms; slice thickness, 3.6 mm; number of excitation, 2; gradient strength, 45 mT/m; scan time, 150 seconds; matrix size, 256 × 256). The b-value of lower diffusion-sensitizing gradient was set at 50 sec/mm² in order to minimize perfusion effects (17). This resulted in significant signal attenuation of vessels, which is called black-blood image (18). The operating console automatically created ADC maps by using the images with b values of 50 and 1000 s/mm². Minimum ADC values were achieved in a point or region of interest (ROI) by measuring the map intensity. In the patients group, the regions with abnormal signal on conventional images were evaluated section by section on high b-value DW images of the same areas. Each region with high signal on the b-1000 image was scrutinized on ADC map to avoid artifacts like T2 shine-through, vessels, non-suppressed fat and other non-pathologic tissues. After evaluating the whole tumoral tissue, we found the minimum ADC value inside the tumor of each patient. In b-1000 images, in normal muscle of the control group, no high signal and no suspicious restricted area was detected. Therefore, no ADC measurement was needed. It is important to note that all images were evaluated by two expert radiologists.

3.4. Histopathological Evaluation

The patients' biopsy materials were investigated by a member of reference pathologists. Osteosarcoma was confirmed after reviewing the slides and histopathological subtype was recorded as well.

3.5. Statistical Analysis

SPSS 20 (IBM Corp. Released 2011, IBM SPSS Statistics for Windows, Version 20.0. Armonk, NY: IBM Corp) was used for statistical analysis. Student t test (unpaired) was performed to compare mean of maximum Cho/Cr ratios in case and control groups. P values less than 0.05 were considered statistically significant. We performed receiver operating curve (ROC) analysis to find the best cut point for maximum Cho/Cr ratio. The area under a curve (AUC) is a measure of predictive power index called concordance, which generated to evaluate the predictive accuracy of Cho/Cr ratio on the probability of having tumoral tissue. A value 0.5 means predictions were no better than random guessing and 1.0 indicating a (theoretically) perfect test (i.e. 100% sensitive and 100% specific). Pearson's correlation analysis and curve fitting were used to evaluate maximum Cho/Cr ratio and minimum ADC value relationship in each patient.

4. Results

4.1. DWI with Measurement of ADC Values

In DW imaging obtained at a b-value 1000 mm²/s of the normal muscle of control group no high signal area suspicious of restriction was visualized. Therefore, no ADC value measurement was needed. We had a reliable dark background of normal muscle in b-1000 images. In this study, the minimum ADC value of patients with osteosarcoma was $0.88 \pm 0.28 \times 10^{-3}$ mm²/s (mean ± SD). ADC values $\leq 1 \times 10^{-3}$ mm²/s were visualized in 14 (82%) of the 17 patients. Signs of restriction are obvious in this range of ADC value by a quick glance to ADC map (Figure 1).

4.2. MRS Finding

In multivoxel proton MR spectroscopy findings of the normal group, there were no statistically significant differences in the maximum Cho/Cr ratios between males (1.37 ± 0.14) and females (1.31 ± 0.44), and between the thigh (1.34 ± 0.07) and the arm (1.33 ± 0.13) (P = 0.361 and P = 0.932). The maximum Cho/Cr ratio and the location of the examination of each normal participant are presented in Table 1.

Table 1. Summary of Proton MR Spectroscopy Results in the Normal Control Group

Control	Maximum Cho/Cr Ratio ^a	Location
1	1.45	Thigh
2	1.36	Thigh
3	1.28	Thigh
4	1.36	Thigh
5	1.35	Thigh
6	1.25	Thigh
7	1.14	Arm
8	1.33	Arm
9	1.57	Arm
10	1.35	Arm
11	1.28	Arm
12	1.34	Arm

^aCholine/ Creatinine ratio.

The maximum Cho/Cr ratio in the tumoral tissue of patients with osteosarcoma was 1.94 ± 1.12 (Figure 2). This ratio in the normal muscle of the normal group reached 1.34 ± 0.11 (Figure 3).

So, the Cho/Cr ratio was significantly higher in osteosarcoma than the normal muscle (P = 0.043) (Figure 4). In spite of significant statistical differences, many of the

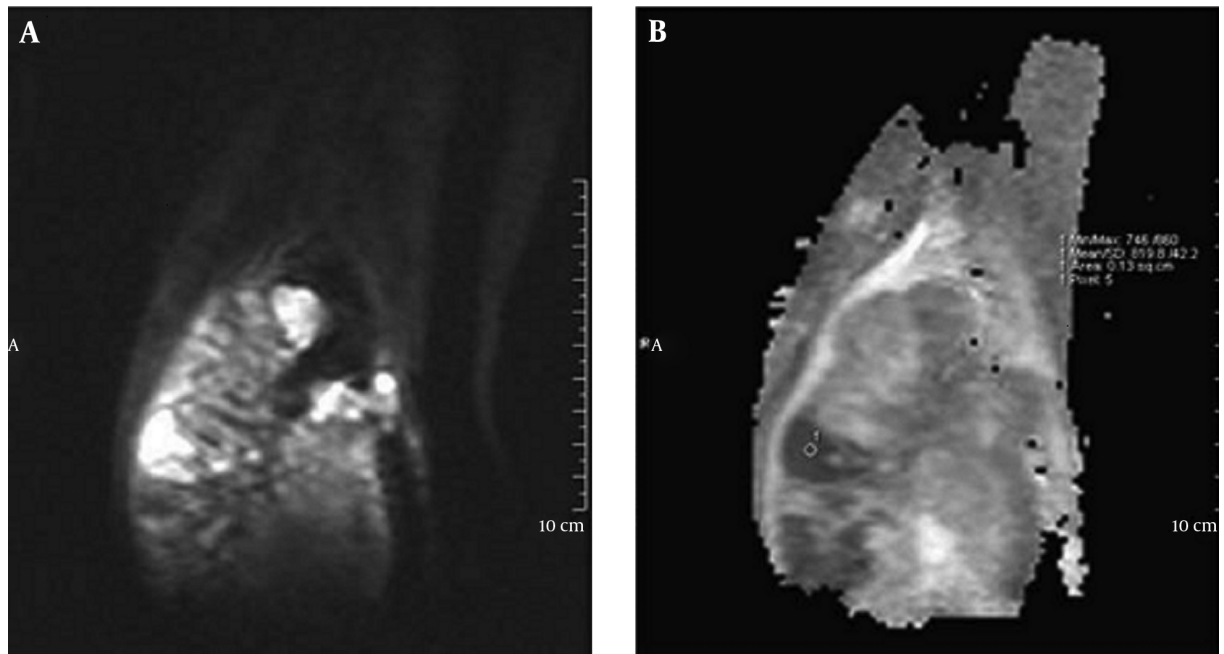


Figure 1. A 20-year-old girl with chondroblastic osteosarcoma of the leg. A, Diffusion weighted (DW) imaging and B, Apparent diffusion coefficient (ADC) map in obvious restriction is present in tumoral tissue. The minimum ADC value is $0.81 \times 10^3 \text{ mm}^2/\text{s}$.

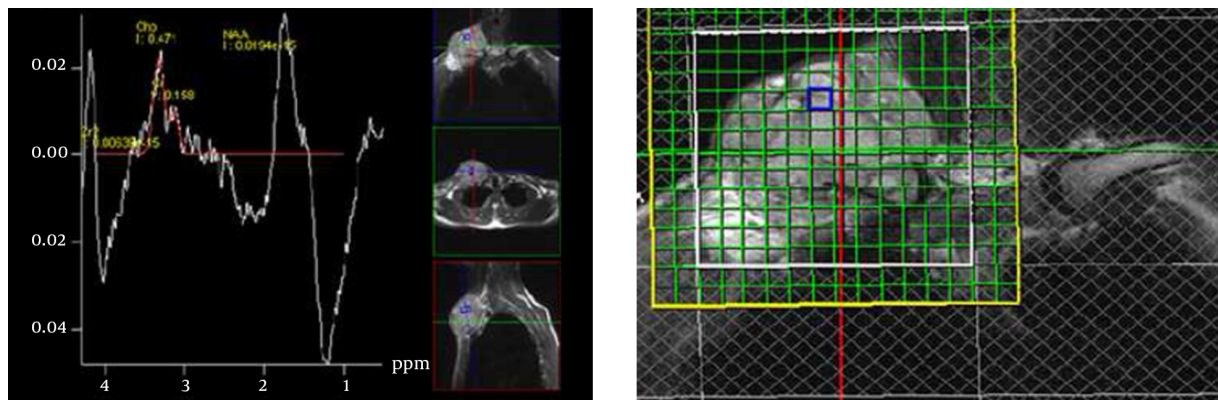


Figure 2. Multivoxel proton MR spectroscopy in a 26-year-old man with small cell osteosarcoma of the clavicle. We had respiratory motions in this place and the spectrum is a little noisy. The maximum choline/creatine (Cho/Cr) ratio of this multivoxel spectrum at visible volume of interest (VOI) is 2.98.

patients had a ratio nearly equal to the ratios of the normal muscle in the normal group. So, we used ROC analysis to assess whether the maximum Cho/Cr ratio could be used in the evaluation of patients with osteosarcoma. The area under the curve (AUC) was 0.7. A maximum Cho/Cr ratio of 1.37 was found to be the cut point with the sensitivity, specificity, and accuracy of 58.8%, 83.3% and 69%, respectively. The maximum Cho/Cr ratio and minimum ADC value for each patient are summarized in [Table 2](#).

After analyzing all patients' data, a significant negative

linear correlation was observed between the maximum Cho/Cr ratios and the minimum ADC values of each patient with a correlation coefficient of -0.544 ($P = 0.024$) ([Figure 5](#)).

4.3. Histopathological Findings

The various histological subtypes of patients with osteosarcoma are summarized in [Table 2](#). It should be noted that although small cell osteosarcoma is a rare subtype of osteosarcoma, we had two cases of this pathology in this

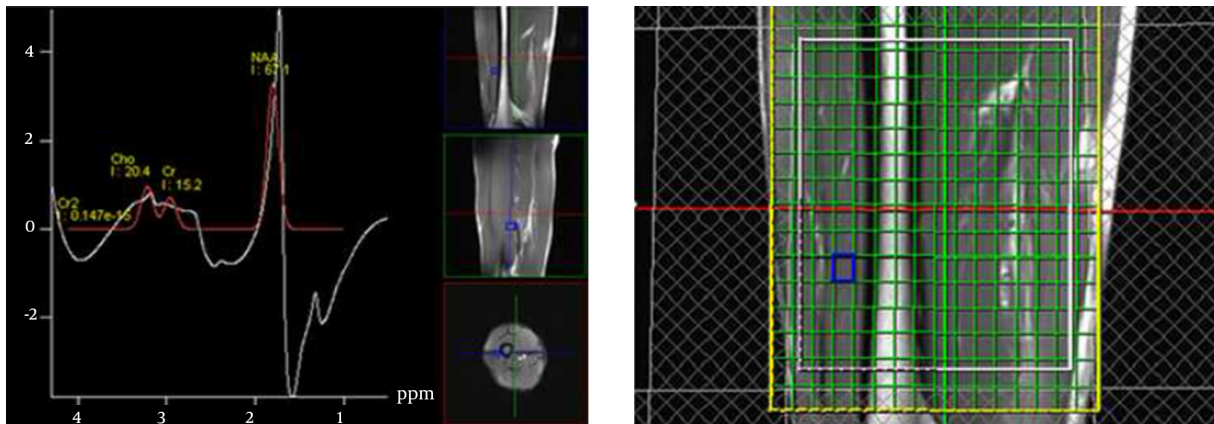


Figure 3. Multivoxel proton MR spectroscopy of the normal muscle of the thigh in a 25-year-old healthy man. The maximum Cho/Cr ratio of this multivoxel spectrum at visible volume of interest (VOI) is 1.2.

Table 2. Summary of Proton MR Spectroscopy and Diffusion Weighted Imaging and Histopathological Subtypes of Patients with Osteosarcoma

Patient ^a	Maximum Cho/Cr Ratio ^b	Minimum ADC Value ^c , $\times 10^{-3} \text{ mm}^2/\text{s}$	Histopathological Subtype
1	1.25	0.80	Chondroblastic
2	1.20	0.81	Chondroblastic
3	1.38	1.30	Chondroblastic
4	2.00	1.00	Chondroblastic
5	5.47	0.45	Small cell
6	2.98	0.61	Small cell
7	3.18	0.75	Fibroblastic
8	1.36	0.59	Fibroblastic
9	1.44	0.83	Osteoblastic
10	1.40	0.82	Pleomorphic
11	1.30	0.96	Periosteal
12	1.28	1.25	Parosteal
13	3.00	0.63	Telangiectatic
14	1.60	0.77	Conventional
15	1.48	0.88	Conventional
16	1.32	1.60	Conventional
17	1.25	0.85	Conventional

^aTwo patients with histopathologic diagnosis other than osteosarcoma were excluded from the study.

^bCholine/ creatinine ratio.

^cApparent diffusion coefficient value.

study. One of them was detected in the clavicle, a relatively less common site of osteosarcoma. Both of them had high Cho/Cr ratios (5.47 and 2.98) and low ADC values (0.45×10^{-3} and $0.61 \times 10^{-3} \text{ mm}^2/\text{s}$, respectively).

5. Discussion

Early diagnosis and determining the tumor boundary provide important insights to prognosis, tumor response to treatment, and quality of life (19).

Proton MR spectroscopy (a metabolic technique) and diffusion weighted imaging (a functional technique) are

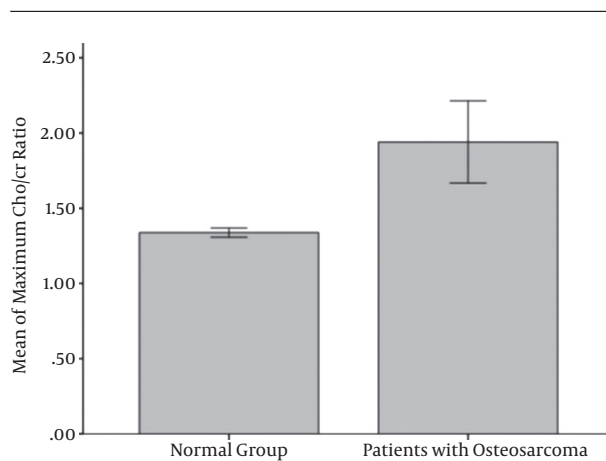


Figure 4. The mean of the maximum Cho/Cr ratio in the normal group and patients with osteosarcoma

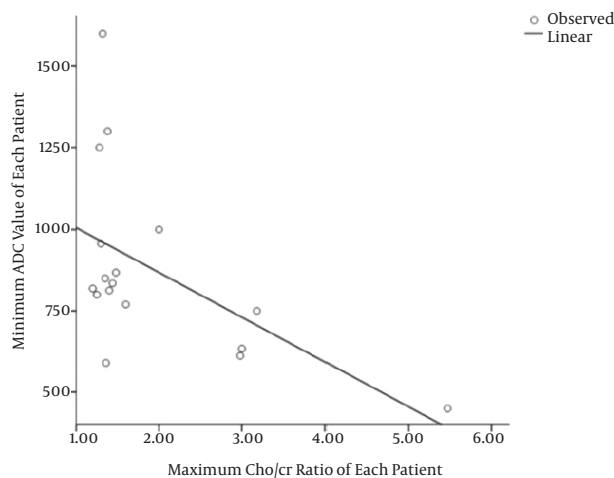


Figure 5. Regression curve of the minimum apparent diffusion coefficient (ADC) value ($\times 10^{-6} \text{ mm}^2/\text{s}$) on the maximum Cho/Cr ratio of each patient with osteosarcoma

two non-invasive and advanced imaging approaches that could be useful in this regard.

In this study, the minimum ADC value of osteosarcoma was $0.88 \pm 0.28 \times 10^{-3} \text{ mm}^2/\text{s}$ (mean \pm SD) and 14 (82%) of the 17 patients had ADC values $\leq 1 \times 10^{-3} \text{ mm}^2/\text{s}$.

The ADC values are comparable with earlier studies on musculoskeletal DW imaging performed at 1.5T.

In a study conducted by Hayashida et al. (20), the mean ADC value of pretreatment was $1.09 \times 10^{-3} \text{ mm}^2/\text{s}$ in treatment responders and $1.35 \times 10^{-3} \text{ mm}^2/\text{s}$ in non-responders.

The minimum ADC values of chondroblastic osteosarcoma and other types of osteosarcoma were reported by Yakushiji et al. as $1.24 \pm 0.10 \times 10^{-3} \text{ mm}^2/\text{s}$ and 0.84 ± 0.15

$\times 10^{-3} \text{ mm}^2/\text{s}$, respectively (21).

Proton MR spectroscopy has been broadly used for detection of malignant lesions in other organs, but there are limited published studies for characterizing musculoskeletal lesions (8, 22, 23) all performed at 1.5 T. We performed 2D proton MR spectroscopy by employing multivoxel technique at 3T during which information is simultaneously obtained over a larger field of view (7). At present, there is only one study in which musculoskeletal investigation was performed on three cases using multivoxel proton MR spectroscopy (24).

In single voxel MR spectroscopic studies, peak of enhancement or solid tissue has been used for voxel placement. Many other tissues like granulation, neovascularized necrosis and inflammatory muscles can show enhancement (25). So, we covered the whole suspicious areas and had to utilize multivoxel technique.

The relationship between the levels of metabolites and the degree of malignancies has been investigated in several studies (23, 24). Metabolite quantification needs an external or internal standard reference, which is usually water. Water content has been affected in different musculoskeletal tissues, several pathological conditions and during treatment that influence the final results of the internal reference methods (7, 26). We employed Cho/Cr ratio to have more reliable numerical results as well as cut point, practically. It has been proved that longer echo times (TEs) increase the Cho/Cr ratio differences between normal and tumoral tissues (8). We used TE of 135 in this study. Herein, maximum Cho/Cr ratio of osteosarcoma (1.94 ± 1.12) was significantly higher than the normal muscle (1.34 ± 0.11). Because of data overlap, we performed ROC curve analysis and acquired 1.37 as the cut point between the normal muscle and osteosarcoma tumoral tissue, with sensitivity, specificity and accuracy of 58.8%, 83.3%, and 69%, respectively.

Doganay et al. (19) reported a sensitivity of 72% and specificity of 83.3% for MR spectroscopy in detecting malignant soft tissue and bone tumors. Lee et al. (12) noted a sensitivity of 68.4% and specificity of 87.5% for proton MR spectroscopy in detecting choline compounds. This sensitivity was lower in primary malignant tumors (53.8%). They had one case of grade 3 osteosarcoma, which did not show any choline compounds due to a relatively large amount of ossification. Although Wang et al. (8) showed high sensitivity and specificity of proton MR spectroscopy in detecting malignant bone and soft tissue tumors in an initial study, in a parosteal osteosarcoma, no choline peak was detected. In a study performed by Qi et al. (27), one patient with osteoblastic osteosarcoma did not show any choline peak either. Low choline concentration (false negative choline uptake) in some subtype of osteosarcoma can be attributed

to lower proton amounts and susceptibility effects due to mineralization (8).

Fayad et al. (5) showed higher choline concentrations in malignant versus benign lesions in a quantitative study. Fayad et al. (28) also showed significant choline concentration in the normal muscle. In a study carried out by Maheshwari et al. (10), the average of Cho/Cr ratio in normal muscle at TEs of 136 and 272 were 1.16 and 1.31, respectively. This emphasizes the maximum Cho/Cr ratio of normal muscle in our study, which is expected to be higher than this average.

Our results appear to be in keeping with previous studies. Utilizing proton MR spectroscopy to evaluate osteosarcoma seems to be potentially successful in about 58.8% of patients.

We had two cases of small cell osteosarcoma, a rare subtype, which is composed of small blue cells, similar to round cell neoplasm as Ewing sarcoma. Both of them showed low ADC values and high Cho/Cr ratios. So, we expect Ewing sarcoma to have the same characteristics, which must be examined in future studies.

Performing DW imaging is technically easier and less time consuming than proton MR spectroscopy. DW imaging was helpful in at least 82% of the patients at a glance, but proton MR spectroscopy was helpful in about 58.8% of the patients. In our study, all patients with Cho/Cr ratios higher than the cut point had ADC values lower than or equal to $1 \times 10^{-3} \text{ mm}^2/\text{s}$ and all patients with the minimum ADC values higher than $1 \times 10^{-3} \text{ mm}^2/\text{s}$ had Cho/Cr ratios lower or nearly in the limit of the cut point. In contrast, some patients with ADC values lower than $1 \times 10^{-3} \text{ mm}^2/\text{s}$ did not show Cho/Cr ratios higher than the cut point. These points reveal that DW imaging is much more effective and proton MR spectroscopy cannot be more helpful than DW imaging in any of the patients with osteosarcoma. However, these results need to be more investigated.

The goal of this study was to search about differences of MR spectroscopy and DWI findings between osteosarcoma and normal muscle. It is clear that in future studies, pathologic correlation of other tissues including necrotic tissues is necessary.

Although osteosarcoma is one of the most frequent primary bone tumors, the number of cases is limited due to its relatively low incidence rate (4 - 5 per year per million persons) (29). So, more and if possible multicenter studies for better evaluation of this aggressive bone tumor should be conducted.

In conclusion, this study reports that performing MR spectroscopy and DW imaging at 3T is helpful in characterizing musculoskeletal lesions. Further evaluation should be performed for pre and post treatment patients. This information could be helpful in increasing diagnostic speci-

ficity of malignancy, definition of the neoadjuvant treatment response, and a preliminary study for determining lesion boundaries.

References

- Xing D, Qasem SA, Owusu K, Zhang K, Siegal GP, Wei S. Changing prognostic factors in osteosarcoma: analysis of 381 cases from two institutions. *Hum Pathol.* 2014;**45**(8):1688-96. doi: [10.1016/j.humpath.2014.04.010](https://doi.org/10.1016/j.humpath.2014.04.010). [PubMed: [24931466](https://pubmed.ncbi.nlm.nih.gov/24931466/)].
- Savage SA, Mirabello L. Using epidemiology and genomics to understand osteosarcoma etiology. *Sarcoma.* 2011;**2011**.
- Wittig JC, Bickels J, Priebe D, Jelinek J, Kellar-Graney K, Shmookler B, et al. Osteosarcoma: a multidisciplinary approach to diagnosis and treatment. *Am Fam Physician.* 2002;**65**(6):1123-32. [PubMed: [11925089](https://pubmed.ncbi.nlm.nih.gov/11925089/)].
- Chung WJ, Chung HW, Shin MJ, Lee SH, Lee MH, Lee JS, et al. MRI to differentiate benign from malignant soft-tissue tumours of the extremities: a simplified systematic imaging approach using depth, size and heterogeneity of signal intensity. *Br J Radiol.* 2014.
- Fayad LM, Wang X, Salibi N, Barker PB, Jacobs MA, Machado AJ, et al. A feasibility study of quantitative molecular characterization of musculoskeletal lesions by proton MR spectroscopy at 3 T. *AJR Am J Roentgenol.* 2010;**195**(1):W69-75. doi: [10.2214/AJR.09.3718](https://doi.org/10.2214/AJR.09.3718). [PubMed: [20566784](https://pubmed.ncbi.nlm.nih.gov/20566784/)].
- Costa FM, Canella C, Gasparetto E. Advanced magnetic resonance imaging techniques in the evaluation of musculoskeletal tumors. *Radiol Clin North Am.* 2011;**49**(6):1325-58. vii-viii. doi: [10.1016/j.rcl.2011.07.014](https://doi.org/10.1016/j.rcl.2011.07.014). [PubMed: [22024301](https://pubmed.ncbi.nlm.nih.gov/22024301/)].
- Deshmukh S, Subhawong T, Carrino JA, Fayad L. Role of MR spectroscopy in musculoskeletal imaging. *Indian J Radiol Imaging.* 2014;**24**(3):210-6. doi: [10.4103/0971-3026.137024](https://doi.org/10.4103/0971-3026.137024). [PubMed: [25114383](https://pubmed.ncbi.nlm.nih.gov/25114383/)].
- Wang CK, Li CW, Hsieh TJ, Chien SH, Liu GC, Tsai KB. Characterization of bone and soft-tissue tumors with in vivo ¹H MR spectroscopy: initial results. *Radiology.* 2004;**232**(2):599-605. doi: [10.1148/radiol.2322031441](https://doi.org/10.1148/radiol.2322031441). [PubMed: [15286325](https://pubmed.ncbi.nlm.nih.gov/15286325/)].
- Abrantes AM, Rio J, Tavares LC, Carvalho RA, Botelho MF. Magnetic resonance spectroscopy in cancer diagnostics. *Oncol Rev.* 2011;**4**(3):177. doi: [10.4081/oncol.2010.177](https://doi.org/10.4081/oncol.2010.177).
- Maheshwari SR, Mukherji SK, Neelon B, Schiro S, Fatterpekar GM, Stone JA, et al. The choline/creatine ratio in five benign neoplasms: comparison with squamous cell carcinoma by use of in vitro MR spectroscopy. *AJNR Am J Neuroradiol.* 2000;**21**(10):1930-5. [PubMed: [11110549](https://pubmed.ncbi.nlm.nih.gov/11110549/)].
- Fayad LM, Barker PB, Bluemke DA. Molecular characterization of musculoskeletal tumors by proton MR spectroscopy. *Semin Musculoskelet Radiol.* 2007;**11**(3):240-5. doi: [10.1055/s-2008-1038313](https://doi.org/10.1055/s-2008-1038313). [PubMed: [18260034](https://pubmed.ncbi.nlm.nih.gov/18260034/)].
- Lee CW, Lee JH, Kim DH, Min HS, Park BK, Cho HS, et al. Proton magnetic resonance spectroscopy of musculoskeletal lesions at 3 T with metabolite quantification. *Clin Imaging.* 2010;**34**(1):47-52. doi: [10.1016/j.clinimag.2009.03.013](https://doi.org/10.1016/j.clinimag.2009.03.013). [PubMed: [20122519](https://pubmed.ncbi.nlm.nih.gov/20122519/)].
- Fayad LM, Jacobs MA, Wang X, Carrino JA, Bluemke DA. Musculoskeletal tumors: how to use anatomic, functional, and metabolic MR techniques. *Radiology.* 2012;**265**(2):340-56. doi: [10.1148/radiol.12111740](https://doi.org/10.1148/radiol.12111740). [PubMed: [23093707](https://pubmed.ncbi.nlm.nih.gov/23093707/)].
- Malek M, Pourashraf M, Mousavi AS, Rahmani M, Ahmadinejad N, Alipour A, et al. Differentiation of benign from malignant adnexal masses by functional 3 tesla MRI techniques: diffusion-weighted imaging and time-intensity curves of dynamic contrast-enhanced MRI. *Asian Pac J Cancer Prev.* 2015;**16**(8):3407-12. [PubMed: [25921153](https://pubmed.ncbi.nlm.nih.gov/25921153/)].
- Khoo MM, Tyler PA, Saifuddin A, Padhani AR. Diffusion-weighted imaging (DWI) in musculoskeletal MRI: a critical review. *Skeletal Radiol.* 2011;**40**(6):665-81. doi: [10.1007/s00256-011-1106-6](https://doi.org/10.1007/s00256-011-1106-6). [PubMed: [21311884](https://pubmed.ncbi.nlm.nih.gov/21311884/)].

16. Oka K, Yakushiji T, Sato H, Hirai T, Yamashita Y, Mizuta H. The value of diffusion-weighted imaging for monitoring the chemotherapeutic response of osteosarcoma: a comparison between average apparent diffusion coefficient and minimum apparent diffusion coefficient. *Skeletal Radiol.* 2010;**39**(2):141-6. doi: [10.1007/s00256-009-0830-7](https://doi.org/10.1007/s00256-009-0830-7). [PubMed: [19924412](https://pubmed.ncbi.nlm.nih.gov/19924412/)].
17. Dudeck O, Zeile M, Pink D, Pech M, Tunn PU, Reichardt P, et al. Diffusion-weighted magnetic resonance imaging allows monitoring of anticancer treatment effects in patients with soft-tissue sarcomas. *J Magn Reson Imaging.* 2008;**27**(5):1109-13. doi: [10.1002/jmri.21358](https://doi.org/10.1002/jmri.21358). [PubMed: [18425832](https://pubmed.ncbi.nlm.nih.gov/18425832/)].
18. Schieda N, Al-Dandan O, El-Khodary M, Shabana W. Low b-value (black blood) respiratory-triggered fat-suppressed single-shot spin-echo echo-planar imaging (EPI) of the liver: comparison of image quality at 1.5 and 3 T. *Clin Radiol.* 2014;**69**(11):1136-41. doi: [10.1016/j.crad.2014.06.017](https://doi.org/10.1016/j.crad.2014.06.017). [PubMed: [25060933](https://pubmed.ncbi.nlm.nih.gov/25060933/)].
19. Doganay S, Altinok T, Alkan A, Kahraman B, Karakas HM. The role of MRS in the differentiation of benign and malignant soft tissue and bone tumors. *Eur J Radiol.* 2011;**79**(2):e33-7. doi: [10.1016/j.ejrad.2010.12.089](https://doi.org/10.1016/j.ejrad.2010.12.089). [PubMed: [21376496](https://pubmed.ncbi.nlm.nih.gov/21376496/)].
20. Hayashida Y, Yakushiji T, Awai K, Katahira K, Nakayama Y, Shimomura O, et al. Monitoring therapeutic responses of primary bone tumors by diffusion-weighted image: Initial results. *Eur Radiol.* 2006;**16**(12):2637-43. doi: [10.1007/s00330-006-0342-y](https://doi.org/10.1007/s00330-006-0342-y). [PubMed: [16909220](https://pubmed.ncbi.nlm.nih.gov/16909220/)].
21. Yakushiji T, Oka K, Sato H, Yorimitsu S, Fujimoto T, Yamashita Y, et al. Characterization of chondroblastic osteosarcoma: gadolinium-enhanced versus diffusion-weighted MR imaging. *J Magn Reson Imaging.* 2009;**29**(4):895-900. doi: [10.1002/jmri.21703](https://doi.org/10.1002/jmri.21703). [PubMed: [19306430](https://pubmed.ncbi.nlm.nih.gov/19306430/)].
22. Oya N, Aoki J, Shinozaki T, Watanabe H, Takagishi K, Endo K. Preliminary study of proton magnetic resonance spectroscopy in bone and soft tissue tumors: an unassigned signal at 2.0-2.1 ppm may be a possible indicator of malignant neuroectodermal tumor. *Radiat Med.* 2000;**18**(3):193-8. [PubMed: [10972550](https://pubmed.ncbi.nlm.nih.gov/10972550/)].
23. Fayad LM, Bluemke DA, McCarthy EF, Weber KL, Barker PB, Jacobs MA. Musculoskeletal tumors: use of proton MR spectroscopic imaging for characterization. *J Magn Reson Imaging.* 2006;**23**(1):23-8. doi: [10.1002/jmri.20448](https://doi.org/10.1002/jmri.20448). [PubMed: [16315208](https://pubmed.ncbi.nlm.nih.gov/16315208/)].
24. Fayad LM, Barker PB, Jacobs MA, Eng J, Weber KL, Kulesza P, et al. Characterization of musculoskeletal lesions on 3-T proton MR spectroscopy. *AJR Am J Roentgenol.* 2007;**188**(6):1513-20. doi: [10.2214/AJR.06.0935](https://doi.org/10.2214/AJR.06.0935). [PubMed: [17515370](https://pubmed.ncbi.nlm.nih.gov/17515370/)].
25. Nelson SJ. Multivoxel magnetic resonance spectroscopy of brain tumors. *Mol Cancer Ther.* 2003;**2**(5):497-507. [PubMed: [12748312](https://pubmed.ncbi.nlm.nih.gov/12748312/)].
26. Michaelis T, Merboldt KD, Bruhn H, Hanicke W, Frahm J. Absolute concentrations of metabolites in the adult human brain in vivo: quantification of localized proton MR spectra. *Radiology.* 1993;**187**(1):219-27. doi: [10.1148/radiology.187.1.8451417](https://doi.org/10.1148/radiology.187.1.8451417). [PubMed: [8451417](https://pubmed.ncbi.nlm.nih.gov/8451417/)].
27. Qi ZH, Li CF, Li ZF, Zhang K, Wang Q, Yu DX. Preliminary study of 3T 1H MR spectroscopy in bone and soft tissue tumors. *Chin Med J (Engl).* 2009;**122**(1):39-43. [PubMed: [19187615](https://pubmed.ncbi.nlm.nih.gov/19187615/)].
28. Fayad LM, Salibi N, Wang X, Machado AJ, Jacobs MA, Bluemke DA, et al. Quantification of muscle choline concentrations by proton MR spectroscopy at 3 T: technical feasibility. *AJR Am J Roentgenol.* 2010;**194**(1):W73-9. doi: [10.2214/AJR.09.3125](https://doi.org/10.2214/AJR.09.3125). [PubMed: [20028894](https://pubmed.ncbi.nlm.nih.gov/20028894/)].
29. Ottaviani G, Jaffe N. *Pediatric and adolescent osteosarcoma*. Springer; 2009. The epidemiology of osteosarcoma.